

## Growth and structure of thin Co films on Cu(111) studied by full-solid-angle x-ray photoelectron distributions

Th. Fauster, G. Rangelov, J. Stober, and B. Eisenhut

*Sektion Physik, Universität München, Schellingstrasse 4, 80799 München, Germany*

(Received 18 May 1993)

Photoelectron spectroscopy at kinetic energies of  $\approx 570$  eV has been performed on a Cu(111) surface with Co coverages of up to 50 monolayers. The angle-integrated data indicate that tall islands develop with Cu atoms in the top layers. The angular distributions of the photoelectrons were measured using a display-type analyzer with an opening angle of  $88^\circ$ . The Co emission patterns always show some threefold symmetry corresponding to the fcc structure of the clean Cu(111) surface. Most of the Co atoms are in the hcp structure and this fraction increases with coverage.

### I. INTRODUCTION

The growth and properties of ultrathin magnetic films are of great technological importance as well as of fundamental interest. The first aspect concerns the development of high-density magnetic storage devices. The latter aspect comprises the question of magnetism in two dimensions<sup>1</sup> and the fabrication of metastable phases of magnetic materials such as iron<sup>2,3</sup> and cobalt.<sup>4-8</sup> Multilayer systems exhibit some fascinating properties, for example, giant magnetoresistive effects<sup>9-12</sup> and oscillations in the magnetic coupling with layer thickness.<sup>9,13-15</sup> Despite the large number of studies, the growth and structure of even the simplest systems are just starting to be understood.<sup>16</sup>

The growth of Co on Cu(111) has been studied with a variety of surface-sensitive techniques. Many authors concluded from their data that the growth was layer by layer,<sup>17-20</sup> which was questioned only recently.<sup>2,12,21</sup> The observation of a sixfold symmetric low-energy electron diffraction (LEED) pattern was interpreted as the growth of Co in the hcp structure. Consequently, the metastable fcc Co phase on Cu(100) (Refs. 4-8) was studied much more than the Co on Cu(111) system. A large number of structural studies of Co/Cu(111) multilayers has been done; however, despite its importance for the magnetic properties, no clear picture has emerged, even though most authors find evidence for Co in fcc as well as hcp surroundings.<sup>22-27</sup>

We have used core-level photoelectron spectroscopy to study the growth and structure of Co on Cu(111). Photoelectrons with a kinetic energy of some hundred electron volts exhibit enhanced intensity along the inter-nuclear axes connecting the emitting atom with its neighbor atoms due to forward scattering.<sup>28-31</sup> The angular distribution of these photoelectrons yields, therefore, structural information which can be interpreted in a straightforward geometrical way. It has been shown by theoretical calculations<sup>32</sup> that it should be possible to determine the stacking sequence of the Co layers on Cu(111).

In Sec. II we will present a short description of the experimental procedures. The results (Sec. III) are presented separately for the angle-integrated x-ray photo-

electron spectroscopy (XPS) intensities and the angular distribution patterns. The discussion in Sec. IV is followed by a short summary and outlook.

### II. EXPERIMENT

The Cu(111) crystal was oriented within  $0.5^\circ$  and was cleaned following standard procedures.<sup>33</sup> The surface cleanliness and crystallographic order were verified with Auger electron spectroscopy and LEED. Co was evaporated from an electron-beam heated wire at a rate of  $\sim 0.01$  monolayers (ML) per second onto the substrate at room temperature and at a pressure of  $< 2 \times 10^{-10}$  mbar. Coverages are given in monolayer equivalents and were determined with an uncertainty of 10% by means of a calibrated quartz microbalance.<sup>34</sup>

For the photoemission experiments the sample was transferred from the preparation chamber to the display-type analyzer<sup>35</sup> under ultrahigh vacuum conditions. Synchrotron radiation with an energy of  $\sim 650$  eV from the HE-TGM-1 beam line of the Berliner Elektronenspeicher-Gesellschaft für Synchrotronstrahlung storage ring was employed to excite the  $3p$  core levels of Co and Cu. The kinetic energies were 578 and 562 eV, respectively. The angular distribution patterns of the photoelectrons were recorded by a two-dimensional display-type electron spectrometer,<sup>35</sup> which allows us to measure simultaneously the complete angular distribution in an acceptance cone of  $88^\circ$ . The data processing and the normalization with respect to the spatial analyzer efficiency have been described previously.<sup>36</sup> The angular intensity distributions are presented in the form of gray-scale pictures in which lighter shading corresponds to higher intensity. In order to show the structures as clearly as possible, the lowest (highest) intensity in each picture is shown black (white).

### III. RESULTS

#### A. Angle-integrated XPS data

Before presenting the angular distribution patterns we are going to discuss some results which can be deduced

directly from the angle-integrated XPS spectra. In Fig. 1 the XPS intensity ratio for the Co and Cu  $3p$  core levels is shown. The data taken at a photon energy of  $\sim 650$  eV were fitted using the spectra for the clean Cu(111) surface and for the 50 ML Co film as reference spectra. The XPS lines are separated by 16 eV so complications due to overlapping lines as in Auger electron spectroscopy are avoided.<sup>5</sup> The fitting procedure adjusted also the inelastic contribution from electrons with lower kinetic energy which have suffered energy losses on their way from the excited atom to the surface. This contribution was assumed to be proportional to the integral of the main elastic peak.<sup>37</sup> The XPS ratio as a function of coverage follows the curve expected for the simultaneous multilayer growth with a Poisson distribution of the terrace areas<sup>38</sup> quite well. However, the mean free path used is 14.3 Å, which is significantly higher than the value of  $\lambda = 9.1$  Å determined for similar kinetic energies for Ag on Pd(111) which grows in a layer-by-layer fashion.<sup>36</sup> A fit of the data of Fig. 1 with a layer-by-layer growth model would require an even larger mean free path. We conclude that the growth mode of Co on Cu(111) certainly cannot be layer by layer and that there must be even more Cu near the surface as in the simultaneous multilayer growth model. One way to achieve this is by building high islands which leave part of the Cu substrate uncovered. An alternative explanation would be segregation or diffusion of Cu atoms to the top layers of the islands. The occurrence of the latter process can be confirmed from the inelastic loss intensity in the top of Fig. 1. The loss signal from Cu  $3p$  electrons decreases with coverage, which can only be explained if a considerable fraction of the Cu atoms are within  $\lambda$  near the surface. Cu atoms covered by Co would show an increase of the inelastic contribution compared to the main line. The inelastic contribution for the Co  $3p$  electrons increases with coverage and reaches its asymptotic value already at a coverage of 1 ML, which would correspond to 2.1 Å. This behavior is compatible with the building of islands

which are considerably higher than expected for the simultaneous multilayer growth. Comparing the inelastic contribution for the Co emission at 0.5 ML coverage to the value for Cu at 15 ML we can get a crude estimate of  $\sim 0.5$  ML of Cu in the top layers, which is also compatible with the corresponding XPS intensities (see Fig. 1). This result is in qualitative agreement with CO-titration measurements<sup>2</sup> which sample only the Cu atoms in the top layer.

## B. Angle-resolved XPS distributions

In Fig. 2(a) we present the Cu  $3p$  angular distribution pattern for a Co coverage of 1.0 ML. There is no significant difference to the pattern of a clean Cu(111) surface (not shown, compare also Ref. 39). In Fig. 2(b) the forward-scattering directions for a fcc(111) surface are plotted in the angular grid of the display-type analyzer. The area of the circles is proportional to the square of the distance between the emitter and the scatterer and roughly corresponds, therefore, to the expected intensity. The numbers give the crystal directions between emitter and scatterer. Enhanced intensity from emitters in the second layer along the  $\langle 110 \rangle$  directions as well as from emitters in the third layer along the  $\langle 112 \rangle$  and  $\langle 310 \rangle$  directions can be clearly identified in Fig. 2.

Figure 2(c) shows the corresponding emission pattern for the Co  $3p$  level. The observation of forward-scattering directions for 1 ML Co coverage rules out a layer-by-layer growth of Co on Cu(111). We cannot, however, distinguish between Co and Cu atoms acting as scatterers above the Co atoms, which would correspond to multilayer growth and segregation or intermixing, respectively. Further Co deposition [Figs. 2(d)–2(f)] leads to an improved signal-to-noise ratio, but does not change the characteristics of the emission pattern significantly. The angular distribution patterns show always a pattern of threefold symmetry<sup>40</sup> with the same orientation as the Cu(111) substrate of Fig. 2(a) even at coverages of 50 ML. Since Co and Cu are close neighbors in the Periodic Table and the  $3p$  core levels of the same symmetry were measured at almost the same kinetic energy, we expect that the emission pattern for fcc Co would be identical to the corresponding pattern for Cu(111). The Co emission patterns are considerably different compared to the clean surface, which proves that the Co films are certainly not pure fcc. Most notably is an outward shift of the  $\langle 110 \rangle$  spots and a relative intensity decrease of the  $\langle 112 \rangle$  spots. Additional intensity appears outside the  $\langle 112 \rangle$  spots where the clean surface exhibits strong minima. The emission pattern appears to become closer to a sixfold symmetric pattern<sup>40</sup> with increasing Co coverage. We note that the emission pattern of 50 ML Co shows a contrast of 0.22 compared to 0.42 for the clean Cu(111) surface. The contrast is defined as the difference between the maximum and the minimum intensity of a pattern normalized to the maximum. The contrast obviously depends on the angular range of the pattern and serves only as a qualitative measure in this context. Note that for the angular distribution patterns in the fig-

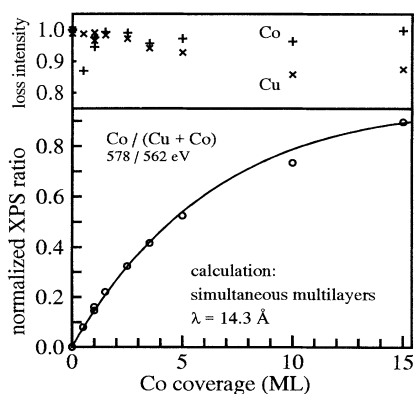


FIG. 1. Bottom: normalized XPS intensity ratio as a function of Co coverage compared to a model calculation for simultaneous multilayer growth (solid line) with the mean free path  $\lambda = 14.3$  Å. Top: normalized inelastic XPS intensity for Co (+) and Cu (x) as a function of coverage.

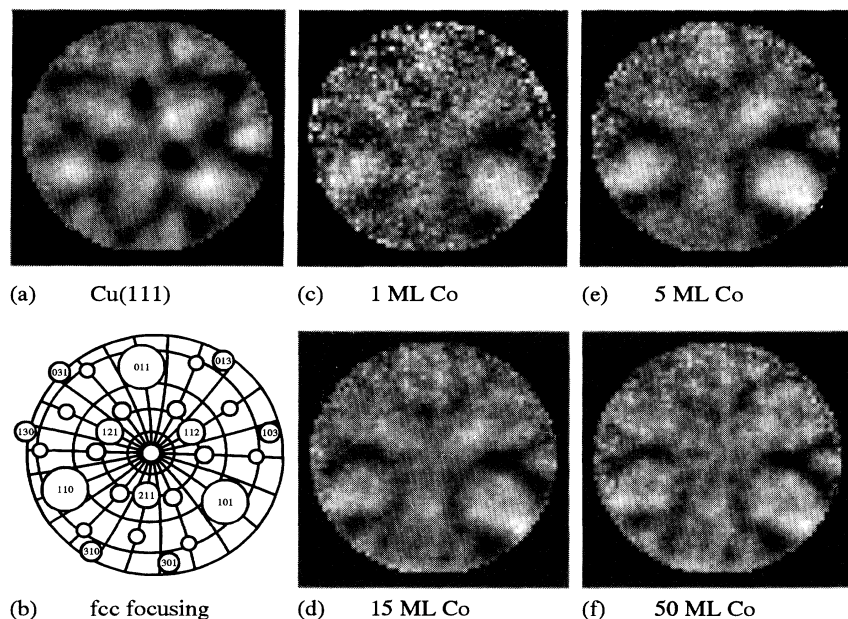


FIG. 2. (a) Experimental angular distribution of Cu 3p photoelectrons (kinetic energy of 562 eV) from a Cu(111) surface covered with 1 ML of Co. (b) Forward-scattering directions for a fcc(111) surface and the angular net of the display analyzer (line separations of  $10^\circ$  and  $15^\circ$  in the polar and azimuthal directions, respectively). (c)–(f) Experimental angular distribution of Co 3p photoelectrons (kinetic energy of 578 eV) from a Cu(111) surface with various coverages of Co.

ures the minimum intensity is shown black and the maximum white in order to show the structures as clearly as possible (see Sec. II). In this way, however, the information about the contrast is lost. It is reflected by the fact that the pattern for clean Cu(111) shows much more pronounced minima and maxima compared to the case of the 50 ML Co film. The reduced contrast of the Co emission patterns indicates that the Co atoms are not in a well-ordered single-phase fcc structure. Instead, there could be both fcc domains [the other one with the pattern of Fig. 2(a) reflected at the horizontal plane] or the hcp structure present. Disordered atoms would not lead to preferred forward-scattering directions and would, therefore, diminish the contrast. The changes of the forward-scattering directions noted above favor the presence of Co atoms in their natural hcp structure.

In order to understand the growth of Co on Cu(111) in more detail we note that we observe a  $(1 \times 1)$  LEED pattern independent of coverage. There is no drastic increase of the background excluding a large amount of disordered atoms. We detected no change of the position of the diffraction spots (at fixed energy) which is in agreement with the small lattice mismatch of  $\sim 3\%$ .<sup>2</sup> The visual inspection of the LEED patterns shows a sixfold symmetry already at low coverages ( $\approx 3$  ML), which has led other authors<sup>17</sup> to the conclusion that Co grows in the hcp phase on Cu(111). This is obviously at variance to the observation of a threefold pattern in photoelectron forward scattering. The observation of a  $(1 \times 1)$  LEED pattern restricts any structural models to the different stacking of hexagonal layers. Keeping in mind that most of the emission and the dominant structures of the angular distribution patterns come from the top three layers (compare the thickness of  $6.3 \text{ \AA}$  to the mean free path of  $9.1 \text{ \AA}$ ) we are left with four different stacking sequences: two fcc structures  $ABC$  and  $ACB$  and two hcp

structures  $ABA$  and  $ACA$ , respectively. Only the relative stacking is important, so we consider the top layer to be  $A$  in all cases. With increasing film thickness the stacking sequence of the top layers is retained for the fcc structure, whereas for the hcp structure we alternate between  $ABA$  and  $BAB$  (which is identical to  $ACA$ , if the top layer is named  $A$ ). No alternating is observed in the emission patterns with increasing layer thickness. This is in agreement with the angle-integrated XPS data which did not confirm a layer-by-layer growth. Therefore, it is plausible that both hcp stacking sequences occur in the top layers with equal probability, leading to a sixfold contribution to the emission patterns.

Figure 3(a) shows the emission pattern for the clean Cu(111) surface rotated  $27^\circ$  to the left compared to Fig. 2(a). The downward pointing triangle from the  $\langle 112 \rangle$  directions can be clearly identified in the left half. In addition is the  $[001]$  forward-scattering direction visible in the top right corner  $55^\circ$  away from the surface normal and  $30^\circ$  above the horizontal meridian. This spot is shown as a gray circle in Fig. 3(b) as are the  $[011]$  and  $[101]$  spots, which appear also as fcc focusing directions in Fig. 2(a). The deposition of Co [Figs. 3(c) and 3(e)] diffuses the  $\langle 112 \rangle$  peaks and more intensity is seen at  $55^\circ$  polar and  $-30^\circ$  azimuthal angle. The  $[001]$  forward-scattering direction comes from an emitter in the second layer and it is, therefore, not possible to distinguish between the fcc and the hcp structure which both can occur in the  $AB$  and  $AC$  stacking of the top layers. The  $[101]$  spot (at  $35^\circ$  polar and  $-30^\circ$  azimuthal angle) appears to be relatively weak compared to the  $[001]$  spot, regardless of its origin from the nearest neighbor in the second layer. The explanation comes from the polarized synchrotron radiation used in this work. The dipole selection rule forbids the primary-electron excitation normal to the polarization vector which lies in the horizontal plane of Figs. 2

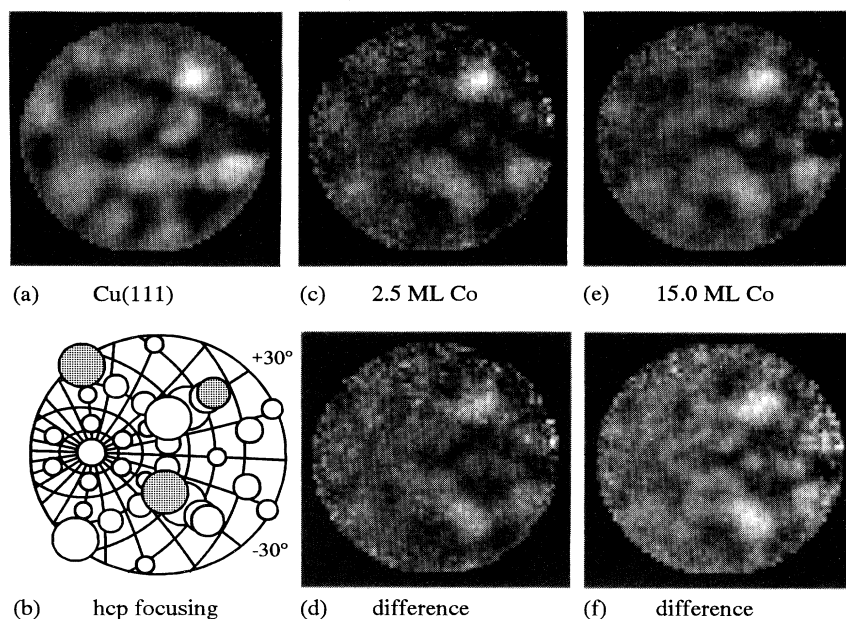


FIG. 3. (a) Experimental angular distribution of Cu  $3p$  photoelectrons (kinetic energy of 562 eV) from a clean Cu(111) surface. The sample is rotated by  $27^\circ$  to the left compared to Fig. 2. (b) Forward-scattering directions for a hcp surface (Ref. 41). The gray circles correspond to emitters in the second layer which are identical for the fcc structure [compare to Fig. 2(b)]. (c) and (e) Experimental angular distribution of Co  $3p$  photoelectrons (kinetic energy of 578 eV) from a Cu(111) surface for Co coverages of 2.5 and 15 ML. (d) and (f) Angular distributions after the subtraction of the fcc component of the pattern.

and 3. This suppresses the  $[101]$  spot in Fig. 3 and leads to a reduction of the intensity of the  $[011]$  and  $[211]$  spot in Fig. 2.

In order to clarify whether the pattern of the Co layers is from two fcc domains with a preferential orientation as the Cu(111) substrate or from a hcp structure we subtracted from the Co pattern a contribution of the fcc Cu(111) pattern. The intensity was chosen carefully so minima (maxima) in the fcc pattern did not lead to maxima (minima) in the difference picture. The result is shown in Figs. 3(d) and 3(f) and exhibits clearly a sixfold symmetry.<sup>40</sup> These patterns cannot be due to a superposition of the emission patterns of two fcc domains of equal intensity since they show minima at  $35^\circ$  polar and  $\pm 30^\circ$  azimuthal angle, where the fcc structure has a clear maximum [compare Fig. 3(a)]. The angular distributions of Figs. 3(d) and 3(f) represent, therefore, the forward-scattering directions of the hcp lattice structure with the possibility of a small contribution from the two fcc domains. Wei, Zhao, and Tong<sup>41</sup> have calculated the emission pattern for a Co(0001) surface for electrons with a kinetic energy of 703 eV, which is close enough to be compared to our measurements at 578 eV since the dominating scattering of the electrons is in forward direction in this energy range.<sup>28-31,41</sup> Their main observation is that due to the zigzag chains of the hcp lattice the forward focusing peaks are broader and that some are actually coalescing.<sup>41</sup> For example, the  $35^\circ$  (fcc  $\langle 110 \rangle$  direction) and  $55^\circ$  (fcc  $\langle 001 \rangle$  direction) peaks from emitters in the third layer combine with a forward focusing peak at  $47^\circ$  of the hcp lattice to form peaks at  $44^\circ$

and  $52^\circ$ , respectively [compare Fig. 3(b)]. The nearest-neighbor direction between layers  $A-A'$  of the hcp lattice should lead to a peak at  $31.5^\circ$  along the horizontal meridian. The atoms in the second layer pull this emission towards  $35^\circ$  (fcc  $\langle 110 \rangle$  direction) leading to two spots which are responsible for the clawlike feature in the emission patterns.<sup>41</sup> The sixfold symmetry of the difference patterns suggests the occurrence of both hcp terminations with equal probability. This is certainly plausible for high coverages. At low coverages the influence of the substrate might be strong enough to induce a preferential termination. Our difference pictures do not indicate any preference, but this might be also due to the subtraction procedure. At low coverages the statistics is not good enough to detect any remaining asymmetries reliably. For quantitative statements a comparison to more detailed calculations would be necessary.

For the determination of the fcc and hcp contribution in the emission patterns we used the following data analysis procedure. Under the assumption that only the Cu(111) fcc structure and the hcp structure contribute to any of the measured patterns, we made a least-square fit by a linear combination of the patterns of Figs. 3(a) and 3(f) using all the data points of the patterns. The results are shown in Fig. 4 as a function of coverage. The fcc contribution is normalized to the sum of the hcp and fcc components of the fit. Since we do not have the data for a hcp Co(0001) surface, there is some uncertainty in the relative normalization of the fcc and hcp patterns. Therefore, the values in Fig. 4 should be regarded only as a qualitative measure for the fcc fraction in the top

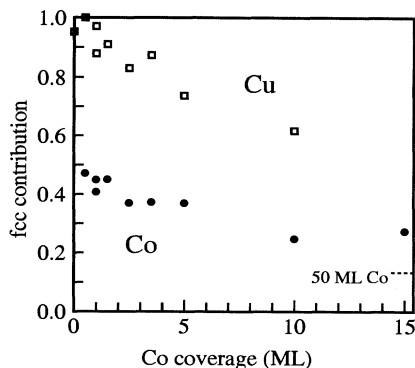


FIG. 4. Contribution from the fcc structure in the emission patterns for Co (filled circles) and Cu (open squares) as a function of coverage.

layers. They show clearly, however, the decrease with coverage for both the Co and the Cu emission. The increasing amount of Cu atoms in a hcp environment could be related to the Cu atoms in the top layers. The electrons emitted from the fcc Cu substrate are attenuated and their emission pattern might be also distorted by the passage through the hcp Co layers.

#### IV. DISCUSSION

The results of the preceding section yield the following information about the growth of Co on Cu(111).

(i) The growth is not layer by layer and is not as simultaneous multilayers with a Poisson distribution of the terrace areas. Instead, relatively tall islands develop with Cu atoms in the top layers.

(ii) The Co films show up to coverages of 50 ML threefold symmetry corresponding to the fcc structure of the clean Cu(111) surface. The remaining Co atoms are in the hcp structure with both terminations (*AB* and *AC*) equally probable.

(iii) The fraction of Co and Cu atoms in the fcc structure in the top layers decreases with coverage in favor of the hcp structure.

These results are in good agreement with the similar study by Kief and Egelhoff<sup>2</sup> using photoelectron and Auger electron forward scattering. These authors, however, measured only in one azimuthal direction away from the surface normal towards the [101] direction. Therefore, conclusions about threefold fcc versus sixfold hcp symmetry cannot be drawn as easily as from our data. Harp *et al.*<sup>12</sup> scanned photoelectron distributions along the same azimuthal direction on a twinned sample. This excludes the possibility to distinguish between threefold and sixfold symmetry, and these authors discuss only the fcc stacking without further justification. Tonner, Han, and Zhang<sup>42</sup> find from their photoelectron forward-scattering data a mixture between fcc and hcp oriented Co for thicker films in agreement with our results. From

the absence of forward scattering in the signal from 1 ML of Co they inferred a layer-by-layer growth. With improved statistics the forward-scattering directions [compare Fig. 2(c)] might have been detected.

For the interpretation of our results, we consider first the predictions for the growth mode of a thin film under equilibrium conditions.<sup>43</sup> The requirement for a layer-by-layer growth to occur is that the sum of the surface free energy of the film plus the interfacial energy must be smaller than the surface free energy of the substrate.<sup>43</sup> The values for the surface free energies<sup>44</sup> of Co (2.7 J/m<sup>2</sup>) and Cu (1.9 J/m<sup>2</sup>) would exclude the layer-by-layer growth in agreement with the observations. The simultaneous multilayer growth would occur if each Co atom hitting the surface stays on the terrace it arrived.<sup>38</sup> This implies that the island edges present a barrier for diffusion. The observation of Cu atoms in the top layers indicates that the surface mobility is high enough to permit diffusion and even intermixing at room temperature. The growth of high islands is confirmed by a recent scanning tunneling microscopy (STM) study.<sup>21</sup> This work reports a double-layer growth at low coverages and the development of tall islands which do not coalesce even at high coverages.

It is tempting to correlate the observation of Co in the fcc structure with the Cu atoms in the top layers. This opens, however, the problem of how the information about the stacking of the substrate is carried to the top layers of the film. One way would be a preferential orientation of the island edges. The STM work,<sup>21</sup> however, found triangular islands with both orientations relative to the substrate in approximately equal proportions. An alternative explanation would be that the fcc Co corresponds to the islands of different appearance growing at step edges.<sup>21</sup> With increasing coverage these step edge islands disappear. This model would imply that the fcc fraction depends on the surface quality. Indeed, Potthast, Voigtländer, and Bonzel<sup>45</sup> have observed sixfold symmetry in XPS forward scattering for Co/Cu(111). A third model would assign the fcc environment to Co atoms close to the Cu substrate. Since the islands observed in STM (Ref. 21) do not coalesce leaving deep trenches between them, it is possible to have some Co atoms at the bottom of the trenches. With increasing Co coverage the number of Co atoms near the interface visible to the electron spectrometer would decrease in agreement with the findings of Fig. 4.

A constant hcp fraction of approximately 35% in the Co layers has been observed in a x-ray scattering study of Co/Cu(111) multilayers with Co layers up to 20 ML thick.<sup>22</sup> This value is somewhat smaller than our results (55–75% hcp fraction in Fig. 4). Apart from the uncertainty in the absolute calibration of the vertical scale of Fig. 4 there are several problems which make a comparison of both experiments difficult. The growth temperature of the multilayers was 50 °C as opposed to room temperature in our study. One cannot exclude a reordering of the Co layers when Cu is deposited on top. The main difference, however, is that the x rays probe the whole sample whereas the photoelectrons come out of the top layers only.

## V. CONCLUSIONS

We have shown that the study of complex structures by photoelectron forward scattering requires the sampling of the angular distributions over the full solid angle,<sup>32,39,46</sup> which can be most easily done with a display-type analyzer. The growth of Co on Cu(111) does not fit into any of the idealized growth modes.<sup>38,43</sup> Defects, stacking faults, diffusion, and segregation<sup>12,20,47</sup> play an important role and are probably the explanation for the wealth of contradictory results in the literature. In this context a study of the growth and structure of the interface at very low coverages using a highly surface-sensitive and element-specific technique such as low-energy ion

scattering<sup>3</sup> seems desirable. We note that the important question about the stacking of the first Co layer with respect to the Cu substrate is still awaiting a conclusive answer.<sup>2</sup> For a better understanding of the multilayer systems more studies of the growth of Cu on Co are needed.<sup>48</sup>

## ACKNOWLEDGMENTS

We acknowledge stimulating discussions with Professor W. Steinmann. This work was supported by the German Federal Minister of Research and Technology, Grant No. BMFT 05 5WMABB 2.

- 
- <sup>1</sup> R. Miranda *et al.*, Phys. Rev. B **25**, 527 (1982).  
<sup>2</sup> M. T. Kief and W. F. Egelhoff, Jr., Phys. Rev. B **47**, 10 785 (1993).  
<sup>3</sup> Th. Detzel, N. Memmel, and Th. Fauster, Surf. Sci. **293**, 227 (1993).  
<sup>4</sup> H. Li and B. P. Tonner, Surf. Sci. **237**, 141 (1990).  
<sup>5</sup> A. Clarke *et al.*, Surf. Sci. **187**, 327 (1987).  
<sup>6</sup> C. M. Schneider *et al.*, Vacuum **41**, 503 (1990).  
<sup>7</sup> D. Kerkmann, D. Pescia, and R. Allenspach, Phys. Rev. Lett. **68**, 686 (1992).  
<sup>8</sup> J. R. Cerdá *et al.*, J. Phys. Condens. Matter **5**, 2055 (1993).  
<sup>9</sup> D. H. Mosca *et al.*, J. Magn. Magn. Mater. **94**, L1 (1991).  
<sup>10</sup> D. Greig *et al.*, J. Magn. Magn. Mater. **110**, L239 (1992).  
<sup>11</sup> J. P. Renard *et al.*, J. Magn. Magn. Mater. **115**, L147 (1992).  
<sup>12</sup> G. R. Harp *et al.*, Phys. Rev. B **47**, 8721 (1993).  
<sup>13</sup> S. S. P. Parkin *et al.*, Phys. Rev. B **46**, 9262 (1992).  
<sup>14</sup> W. F. Egelhoff, Jr. and M. T. Kief, Phys. Rev. B **45**, 7795 (1992).  
<sup>15</sup> M. T. Johnson *et al.*, Phys. Rev. Lett. **69**, 969 (1992).  
<sup>16</sup> R. Miranda, Appl. Phys. (to be published).  
<sup>17</sup> L. Gonzalez *et al.*, Phys. Rev. B **24**, 3245 (1981).  
<sup>18</sup> R. Miranda *et al.*, Surf. Sci. **117**, 319 (1982).  
<sup>19</sup> P. Roubin, D. Chandresis, G. Rossi, and J. Lecante, J. Phys. F **18**, 1165 (1988).  
<sup>20</sup> Q. Chen, M. Onellion, and A. Wall, Thin Solid Films **196**, 103 (1991).  
<sup>21</sup> J. de la Figuera, J. E. Prieto, C. Ocal, and R. Miranda, Phys. Rev. B **47**, 13 043 (1993).  
<sup>22</sup> F. J. Lamelas *et al.*, Phys. Rev. B **40**, 5837 (1989).  
<sup>23</sup> K. Le Dang *et al.*, Phys. Rev. B **41**, 12 902 (1990).  
<sup>24</sup> H. A. M. de Gronckel *et al.*, Phys. Rev. B **44**, 9100 (1991).  
<sup>25</sup> C. Mény, P. Pannisod, and R. Loloe, Phys. Rev. B **45**, 12 269 (1992).  
<sup>26</sup> J. C. S. Kools, R. Coehoorn, F. J. G. Hakkens, and R. J. H. Fastenau, J. Magn. Magn. Mater. **121**, 83 (1993).  
<sup>27</sup> S. Pizzini *et al.*, J. Magn. Magn. Mater. **121**, 208 (1993).  
<sup>28</sup> W. F. Egelhoff, Jr., CRC Crit. Rev. Solid State Mater. Sci. **16**, 213 (1990).  
<sup>29</sup> J. Osterwalder, Arab. J. Sci. Engin. **15**, 273 (1990).  
<sup>30</sup> C. S. Fadley, in *Synchrotron Radiation Research: Advances in Surface Science*, edited by R. Z. Bachrach (Plenum, New York, 1992), Chap. 11.  
<sup>31</sup> S. A. Chambers, Adv. Phys. **40**, 357 (1991).  
<sup>32</sup> C. M. Wei, T. C. Zhao, and S. Y. Tong, Phys. Rev. Lett. **65**, 2278 (1990).  
<sup>33</sup> R. Schneider, H. Dürr, Th. Fauster, and V. Dose, Phys. Rev. B **42**, 1638 (1990).  
<sup>34</sup> G. Rangelov, P. Augustin, J. Stober, and Th. Fauster (unpublished).  
<sup>35</sup> D. Rieger, R. D. Schnell, W. Steinmann, and V. Saile, Nucl. Instrum. Methods **208**, 777 (1983).  
<sup>36</sup> B. Eisenhut, J. Stober, G. Rangelov, and Th. Fauster, Phys. Rev. B **47**, 12 980 (1993).  
<sup>37</sup> D. A. Shirley, Phys. Rev. B **5**, 4709 (1972).  
<sup>38</sup> C. Argile and G. E. Rhead, Surf. Sci. Rep. **10**, 277 (1989).  
<sup>39</sup> Z.-L. Han *et al.*, Surf. Sci. **258**, 313 (1991).  
<sup>40</sup> Strictly speaking, the emission patterns have only a twofold symmetry (reflection about a vertical plane) due to the polarized nature of the synchrotron radiation. This is further reduced by the distortions of the ellipsoidal analyzer (Ref. 35). A sixfold pattern as opposed to a threefold pattern would be symmetric under a reflection about a horizontal plane.  
<sup>41</sup> C. M. Wei, T. C. Zhao, and S. Y. Tong, Phys. Rev. B **43**, 6354 (1991).  
<sup>42</sup> B. P. Tonner, Z.-L. Han, and J. Zhang, Phys. Rev. B **47**, 9723 (1993).  
<sup>43</sup> E. Bauer, Z. Kristallographie **110**, 372 (1958); Appl. Surf. Sci. **11/12**, 479 (1982).  
<sup>44</sup> L. Z. Mezey and J. Giber, Jpn. J. Appl. Phys. **21**, 1569 (1982).  
<sup>45</sup> K. Potthast, B. Voigtländer, and H. P. Bonzel (unpublished).  
<sup>46</sup> J. Osterwalder, T. Greber, A. Stuck, and L. Schlapbach, Phys. Rev. B **44**, 13 764 (1991).  
<sup>47</sup> G. J. Mankey, R. F. Willis, and F. J. Himpsel, Phys. Rev. B **47**, 190 (1993).  
<sup>48</sup> D. Hartmann *et al.*, J. Magn. Magn. Mater. **121**, 160 (1993).

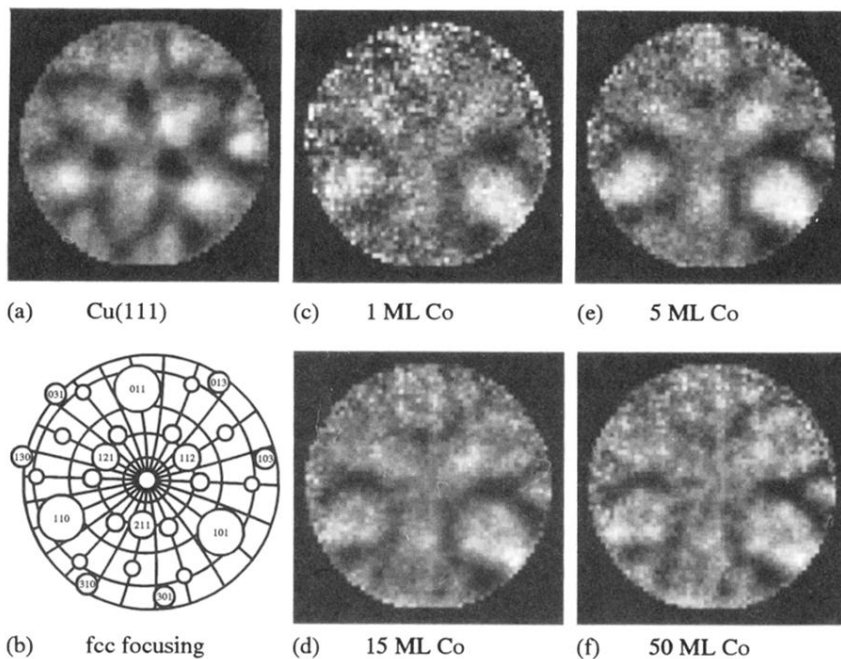


FIG. 2. (a) Experimental angular distribution of Cu 3p photoelectrons (kinetic energy of 562 eV) from a Cu(111) surface covered with 1 ML of Co. (b) Forward-scattering directions for a fcc(111) surface and the angular net of the display analyzer (line separations of  $10^\circ$  and  $15^\circ$  in the polar and azimuthal directions, respectively). (c)–(f) Experimental angular distribution of Co 3p photoelectrons (kinetic energy of 578 eV) from a Cu(111) surface with various coverages of Co.

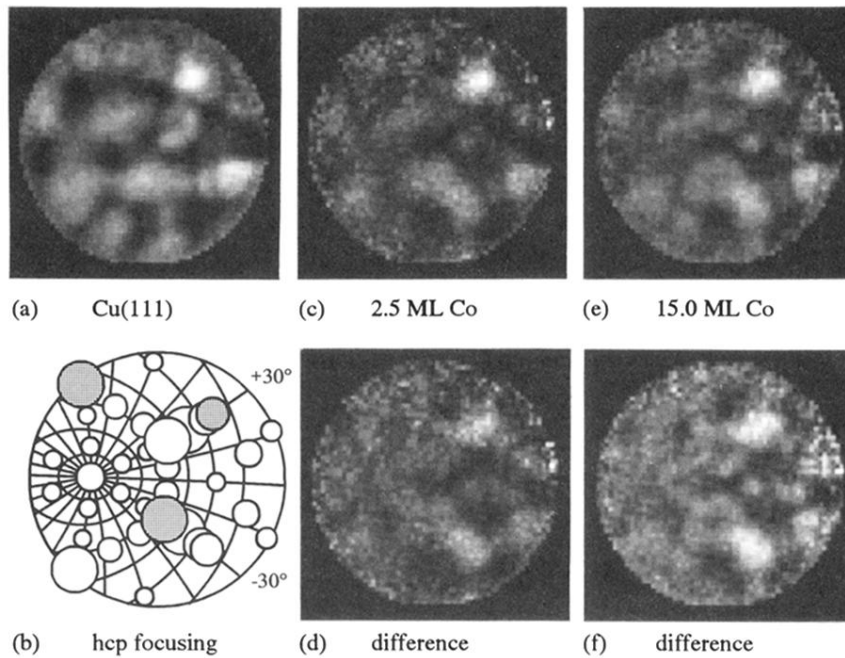


FIG. 3. (a) Experimental angular distribution of Cu  $3p$  photoelectrons (kinetic energy of 562 eV) from a clean Cu(111) surface. The sample is rotated by  $27^\circ$  to the left compared to Fig. 2. (b) Forward-scattering directions for a hcp surface (Ref. 41). The gray circles correspond to emitters in the second layer which are identical for the fcc structure [compare to Fig. 2(b)]. (c) and (e) Experimental angular distribution of Co  $3p$  photoelectrons (kinetic energy of 578 eV) from a Cu(111) surface for Co coverages of 2.5 and 15 ML. (d) and (f) Angular distributions after the subtraction of the fcc component of the pattern.